Main Manuscript for

A patchwork pathway of apparently recent origin enables degradation of the synthetic buffer compound TRIS in bacteria.

Johannes Holert[1*], Aron Borker[1], Laura Nübel[1], Rolf Daniel[2], Anja Poehlein[2], Bodo Philipp[1,3*]

[1] Institute for Molecular Microbiology and Biotechnology, Microbial Biotechnology & Ecology group, University of Münster, Münster, Germany

[2] Institute for Microbiology and Genetics, University of Göttingen, Göttingen, Germany

[3] Environmental Microbiology, Fraunhofer Institute for Molecular Biology and Applied Ecology, Schmallenberg, Germany

* Corresponding authors: Johannes Holert, Bodo Philipp

Email: johannes.holert@uni-muenster.de

Author Contributions: JH conceived the study, designed, planned, and performed experiments, supervised the work, analysed data, and wrote the manuscript. AB performed cloning, conjugation, and isolation experiments and analysed data. LN performed isolation and growth experiment and analysed data. RD contributed reagents and analytic tools. AP performed DNA and RNA extractions, library preparation, DNA sequencing, and transcriptome analysis, and edited the manuscript. BP conceived the study, supervised the work, co-wrote the manuscript, and supplied funding.

Competing Interest Statement: The authors declare no conflict of interest.

Classification: Biological Sciences/Microbiology

Keywords: TRIS, bacterial catabolism, pathway evolution, horizontal gene transfer, Pseudomonas

This PDF file includes:

Main Text
Figures 1 to 5
Tables 1 to 2

Abstract

The widely used synthetic chemical 2-amino-2-hydroxymethyl-propane-1,3-diol (TRIS) was long considered to be biologically inert. Herein, we describe a complete degradation pathway for the catabolism of TRIS in bacteria. By serendipity, *Pseudomonas hunanensis* Teo1 was isolated from sewage sludge and shown to be able to grow with TRIS as only carbon and nitrogen source. Genome sequencing and transcriptome analyses revealed two adjacent gene clusters embedded in a mobile genetic element on a conjugative plasmid to be upregulated during growth with TRIS. Conjugational transfer of this plasmid into *P. putida* KT2440 enabled this strain to grow with TRIS confirming that these clusters encode the complete TRIS degradation pathway. Heterologous gene expression in *Escherichia coli* revealed cluster I to encode a TRIS uptake protein, a TRIS dehydrogenase, and a TRIS aldehyde dehydrogenase, which catalyze the oxidation of TRIS into 2-hydroxymethylserine. Phylogenetic analysis suggests that the TRIS dehydrogenase proteins evolved from choline dehydrogenases. Genes encoded in cluster II encode a methylserine hydroxymethyltransferase and a D-serine dehydratase which could plausibly catalyze conversion of 2-hydroxymethylserine into pyruvate. Subsequent enrichments from wastewater purification systems led to the isolation of further TRIS-degrading bacteria from the *Pseudomonas* and *Shinella* genera which all carried the respective gene clusters in a similar genetic context as strain Teo1.

Our data indicate that TRIS degradation evolved by gene assembly and enzyme adaptation from multiple independent metabolic pathways. Genomic database searches showed that TRIS degradation is now globally distributed, confirming its dissemination by horizontal gene transfer.

Significance statement

TRIS is a synthetic organic chemical that has been mass-produced since the 1950s and is now used in countless applications in industry, medicine, and households world-wide, in parts due to its presumed biological inertness. Our results challenge this common conception, showing that TRIS is biologically degradable by an apparently recently evolved pathway, providing insight into the evolution of metabolic pathways that make such ubiquitous chemicals available as growth substrates for bacteria. Such knowledge is valuable for developing new processes of wastewater purification in times of increasing water scarcity.

Introduction

Since the beginning of the industrial revolution hundreds of thousands of new pesticides, herbicides, medical drugs, and other industrial chemicals were synthesized to meet the growing demand of newly emerging agricultural, pharmaceutical, and industrial applications (1). Many of these anthropogenic chemicals eventually end up in the environment, where their removal is initially restricted due to the absence of efficient biological degradation mechanisms. However, more and more degradation pathways for chemicals that were introduced in the early twentieth century are now being discovered in microbes, suggesting that functional mineralization pathways can evolve within decades after the initial exposure of the microbial community (2). A prominent example is the degradation pathway for the anthropogenic herbicide atrazine, which has evolved in the genus *Pseudomonas* around fifty years after the large scale introduction of atrazine to the market, enabling these bacteria to exploit this compound as a carbon and nitrogen source for growth (3). Similarly, catabolic mineralization pathways for other industrially relevant compounds that were introduced in the early twentieth century including herbicides, pesticides, food additives, and medical drugs are now found in different microorganisms isolated from habitats exposed to these chemicals (4–8). Here, novel pathways can evolve as a result of sufficient positive selective pressure for either the detoxification of such chemicals or their use as a new nutrient source (2). Typically, novel degradation pathways emerge in a process called patchwork assembly by the recruitment, adaptation, and mutation of one or more genes encoding promiscuous enzymes from other metabolic pathways, either from within the host organism via gene duplication or via horizonal gene transfer (HGT) from the microbial community (1, 2, 9). If the mutations happen to increase the substrate affinity and catalytic activity towards the respective new substrate and if the new catalytic activity enables the host to transform the new substrate into metabolites of an already existing metabolic pathway, it will gain a selective advantage over competing microbes by being able to use this compound as a new nutrient and energy resource (1, 2). The genetic information encoding such novel catabolic pathways is often located on mobile genetic elements, such as plasmids or transposons, enabling transfer of the novel pathway to other microbes via HGT (4, 10, 11). Eventually, positive selection for the new catabolic trait can lead to a loss of mobility and manifestation of the new pathway in the genome of its host.

However, the environmental concentrations of synthetic compounds may be too low to provide enough selection pressure for the evolution of novel catabolic pathways. Especially in

66 wastewater treatment plants where the availability of other, readily degradable organic
67 compounds is high, many low-concentrated synthetic compounds presumably reside too
68 shortly for the evolution of novel degradation pathways and remain in the purified wastewater
69 as so-called micropollutants (12, 13). Even some synthetic and natural compounds for which
70 efficient biodegradation pathways exist, such as steroid hormones, are sometimes not fully
71 metabolized in wastewater treatment plants due to their low concentration and contribute to the
72 micropollutant pool. To enhance the biodegradation of such micropollutants, bioaugmentation
73 of water treatment facilities is increasingly being considered, which implies the establishment
74 of microorganisms in the water purification processes, which have been isolated for their ability
75 to efficiently degrade the respective organic compounds (14, 15).
76 The study presented here was originally set up to isolate bacteria capable of degrading
77 steroid hormones in low concentrations from activated sludge. To increase the chances of
78 isolating strains that can later be established for bioaugmentation in real wastewater treatment
79 plant conditions, we used an artificial wastewater medium to mimic typical wastewater nutrient
80 conditions. Surprisingly, our enrichment procedure resulted in the isolation of a bacterial strain
81 that did not grow with the provided steroid hormones, but with the synthetic medium buffer
82 TRIS (2-amino-2-(hydroxymethyl)propane-1,3-diol). Herein, we pursued this finding further
83 and present the identification and characterization of a bacterial degradation pathway for TRIS,
84 which has been considered to be biologically inert so far.
85

86 # Results

87 ## Isolation and characterization of the TRIS-degrading strain *Pseudomonas hunanensis* Teo1

88 The first TRIS-degrading organism was isolated from an enrichment culture that was
89 originally designed to isolate testosterone-degrading bacteria from activated sludge (**Supp.**
90 **Methods**). We repeatedly observed growth in the enrichment cultures in TRIS-buffered
91 artificial wastewater medium without removal of the provided carbon source testosterone (not
92 shown). Plating of the enrichment cultures onto solid medium containing testosterone resulted
93 in the isolation of a bacterial strain that was not able to grow with testosterone but showed
94 growth in liquid artificial wastewater medium without the addition of any extra carbon or
95 nitrogen source. Subsequent growth experiments in phosphate buffered minimal medium with
96 different concentrations of TRIS confirmed a linear relationship between the provided TRIS
97 concentration and the amount of biomass produced by the isolate (**Fig. 1A**), suggesting that
98 TRIS was the growth substrate in these cultures. Growth experiments coupled with HPLC-MS
99 analysis confirmed that TRIS was completely removed from the culture medium, suggesting
100 its utilization as a carbon and nitrogen source for growth (**Fig. 1B-D**). The only detectable
101 metabolite accumulating in the medium was ammonium, with around 40 % of the nitrogen
102 introduced with the TRIS substrate being released as ammonium into the medium (**Fig. 1C-**
103 **D**). Strain Teo1 was not able to use the structurally similar amino alcohols serinol, 2-amino-2-
104 methyl-1-propanol, and 2-amino-2-methyl-1,3-propanediol as growth substrates (**Supp. Fig.**
105 **S1**), while it was able to use the quaternary ammonium compounds choline and betaine, and
106 the secondary amine sarcosine as substrates. It further grew with the amino acids D- and L-
107 serine, but not with glycine. Based on its whole genome sequence (**Supp. Methods**), the isolate
108 was taxonomically classified as a representative of the species *Pseudomonas hunanensis* and
109 was named strain Teo1 (**Supp. Tab. ST1**). The genome of strain Teo1 consists of a circular
110 chromosome (6.13 Mbp) and two large, circular plasmids, p1_Teo1 (156.3 kbp) and p2_Teo1
111 (65.0 kbp).

112 ## Identification of TRIS degradation genes

113 TRIS growth experiments and time-resolved analysis of TRIS degradation in cell
114 suspensions of strain Teo1 showed that Tris degradation was induced in cells pre-grown with
115 TRIS while it was not induced in pyruvate pre-grown cells (**Supp. Fig. S2**), suggesting that
116 TRIS catabolism is regulated at the transcriptional level in strain Teo1. Based on this
117 observation we used transcriptomics to identify potential TRIS degradation genes by

118 quantifying mRNA levels in TRIS-grown and pyruvate-grown Teo1 cells. A total of 398 genes
119 were differentially regulated in TRIS- compared to pyruvate-grown cells (fold change (FC) >
120 4, $p_{adj} < 0.05$, **Fig. 1E**, **Dataset SD1**), of which 65 were upregulated in TRIS-grown cells. Ten
121 of the twelve most upregulated genes in TRIS-grown cells were found in two adjacent gene
122 clusters (**Fig. 1E-G**) localized on the p1_Teo1 plasmid. The genes in cluster I were annotated
123 as a putative solute binding protein, an amino acid/polyamine-like transporter protein, a choline
124 dehydrogenase-like protein, a NAD/NADP-dependent aldehyde dehydrogenase, a Δ(1)-
125 pyrroline-2-carboxylate/Δ(1)-piperideine-2-carboxylate reductase-like protein, and an alpha-
126 ketoglutaric semialdehyde dehydrogenase-like protein (**Tab. 1**). The genes in cluster II were
127 annotated as a serine hydroxymethyltransferase-like protein, a D-serine dehydratase-like
128 protein, and two proteins presumably involved in the transformation of methylene
129 tetrahydrofolate into tetrahydrofolate and formate. The clusters are separated by a gene that
130 encodes a helix-turn-helix (HTH)-type transcriptional regulator. Based on the similar
131 upregulation of their genes, both gene clusters appear to be expressed as operons (**Fig. 1G**).
132 Due to their strong upregulation and their colocalization in putative operons we proposed that
133 these genes or a subset of them are involved in TRIS degradation in strain Teo1.

134 Characterization of the initial TRIS degradation reactions

135 Based on the predicted protein functions encoded in the upregulated gene clusters, we
136 hypothesized that TRIS is initially oxidized by the proteins encoded in cluster I. To test this,
137 we cloned combinations of the genes encoding the putrescine importer-like protein, the choline
138 dehydrogenase-like protein and the aldehyde dehydrogenase into the expression plasmid
139 pUCp18, transformed the plasmids into *E. coli*, and tested high density cell suspensions of the
140 resulting strains for TRIS transformation activity. While the *E. coli* strains that carry only the
141 putrescine importer gene or the choline and aldehyde dehydrogenase genes did not transform
142 TRIS, the strain with all three genes transformed TRIS almost completely into a new compound
143 within 24 h (**Fig. 2A**). This compound was identified as 2-hydroxymethylserine (**Fig. 2B**) based
144 on its molecular weight, which was 14 Da heavier than that of TRIS, suggesting the oxidation
145 of one hydroxymethyl group into a carboxylic group. To test whether this presumable TRIS
146 degradation intermediate can be further utilized by strain Teo1, sterilized culture supernatants
147 containing 2-hydroxymethylserine were used as growth medium for Teo1, confirming that
148 strain Teo1 can grow with and fully degrade 2-hydroxymethylserine (**Fig. 2C**). These results
149 supported our hypothesis that TRIS is transported into the cells by the putrescine importer-like
150 protein and subsequently oxidized by the choline dehydrogenase-like protein and the aldehyde

151 dehydrogenase. Thus, we propose that these genes encode a TRIS uptake protein (TupA), and
152 two TRIS-oxidizing proteins, namely a TRIS dehydrogenase (TopA) and a TRIS aldehyde
153 dehydrogenase (TopB).

154 Isolation of further TRIS-degrading bacteria and genomic analysis of TRIS degradation

155 Subsequent targeted enrichment of TRIS-degrading bacteria resulted in the isolation of
156 seven *Pseudomonas* strains (Teo2, Teo3, Teo4, Teo6, Teo8, Teo10, and Teo11) and one
157 *Shinella zoogloeoides* strain (Teo12) (**Supp. Tab. ST1**). All isolates were all able to grow with
158 TRIS as only carbon and nitrogen source and completely removed TRIS from the culture
159 medium (**Supp. Fig. S3**). The *Pseudomonas* strains Teo2, Teo4, Teo6, Teo8, and Teo11 and
160 the *Shinella* isolate strain Teo12 were isolated from different municipal wastewater treatment
161 plant samples, *Pseudomonas sichuanensis* Teo3 from an activated charcoal basin of a water
162 purification plant, and *Pseudomonas* sp. strain Teo10 from a freshwater lake sample.
163 Enrichment cultures from two additional wastewater treatment plants and from five freshwater
164 habitats did not develop growth (**Supp. Tab. ST1)**.
165 We sequenced the genomes of five *Pseudomonas* isolates (**Supp. Methods**) and found
166 homologous TRIS degradation gene clusters to the ones identified in strain Teo1 in all of these
167 strains (**Fig. 3, Suppl. Fig. S4**). In *Pseudomonas* strains Teo2, Teo4, Teo6, and Teo8 the
168 clusters are also localized on plasmids (p1_Teo2, p1_Teo4, p1_Teo6, and p2_Teo8) and the
169 plasmids have high similarities to p1_Teo1 (**Fig. 3A**). In *Pseudomonas* strain Teo3, the clusters
170 are encoded in the chromosome (**Fig. 3B**). While all gene clusters II are highly similar, only
171 the *tupA*, *topA*, and *topB* genes are conserved in all cluster I sequences (**Fig. 3, Suppl. Fig. S4**),
172 suggesting that the Δ(1)-pyrroline-2-carboxylate/Δ(1)-piperideine-2-carboxylate reductase-
173 like protein and the alpha-ketoglutaric semialdehyde dehydrogenase-like protein are not
174 required for TRIS degradation. In all these strains, the TRIS degradation gene clusters are
175 flanked by sequences similar to known bacterial insertion elements (**Fig. 3B**), suggesting that
176 the TRIS degradation gene clusters are located within a mobile genetic element (11). A search
177 in the NCBI nucleotide database identified one *Priestia* genome (accession CP065422.1) and
178 three *Pseudomonas* genomes (CP069081.1, CP097105.1, CP114115.1) with homologous gene
179 clusters **(Fig. 3A, Suppl. Fig. S4)**. In *Priestia*, and two of the *Pseudomonas* strains the clusters
180 are also plasmid-borne, while they are encoded chromosomally in *Pseudomonas* sp. strain
181 GXZC (**Fig. 3B**).
182 We also sequenced the genome of the *Shinella* isolate (**Supp. Methods**), which consists of
183 one circular chromosomes (3.54 Mbp) and three circular plasmids, p1_Teo12 (1.89 Mbp),

184 p2_Teo12 (221.54 kbp) and p3_Teo12 (140.01 kbp), which have no apparent similarity to the
185 TRIS degradation-encoding *Pseudomonas* plasmids. However, a DNA region on p2_Teo12
186 encodes homologs of all TRIS degradation genes in two adjacent gene clusters, except for the
187 genes encoding the solute binding protein, the uptake protein TupA, the Δ(1)-pyrroline-2-
188 carboxylate/Δ(1)-piperideine-2-carboxylate reductase-like protein, and the alpha-ketoglutaric
189 semialdehyde dehydrogenase-like protein (**Fig. 3B, Suppl. Fig. S4**). In these clusters, the *topA*
190 and *topB* gene homologs are encoded in the same orientation as in cluster I of the *Pseudomonas*
191 TRIS degradation gene clusters, while the genes are differently oriented in cluster II. A
192 homologous regulator gene to the one found in the *Pseudomonas* gene clusters is located
193 upstream of this cluster. A search in the NCBI nucleotide database identified a closely related
194 *Rhizobium oryzihabitans* strain M15 (CP048637.1), that carries a homologous DNA segment
195 on a plasmid (p5, **Fig. 3B**). The predicted TRIS degradation gene clusters in *S. zoogloeoides*
196 *Teo12* and strain M15 are separated by a truncated transposase gene and flanked by additional
197 transposase genes and insertion elements.
198 A phylogenetic analysis of the TopA proteins with closely related proteins of the glucose-
199 methanol-choline oxidoreductase family (GMC, InterPro IPR012132) revealed that the TopA
200 proteins form a unique cluster that diverges from a clade containing choline dehydrogenase
201 protein sequences (**Supp. Fig. S5A**). In contrast, other choline dehydrogenase proteins of the
202 TRIS-degrading isolates encoded outside of the TRIS degradation gene clusters cluster within
203 the choline dehydrogenase clade, except for two choline dehydrogenase proteins from *S.*
204 *zoogloeoides Teo12*, which cluster at the base of the TopA cluster. A phylogenetic analysis of
205 the TopB proteins with closely related proteins containing an aldehyde dehydrogenase domain
206 (InterPro IPR015590**)** showed that the TopB proteins also from a distinct cluster within the
207 dataset with closest relations to a reviewed aldehyde dehydrogenase (PuuC, Accession P23882)
208 that oxidizes aldehydes during putrescine catabolism in *E. coli* (**Supp. Fig. S5B**). Other PuuC-
209 like proteins encoded outside of the TRIS degradation gene clusters of the TRIS-degrading
210 isolates cluster in close proximity to the TopB cluster.

211 Conjugational transfer of TRIS degradation plasmids

212 The TRIS degradation-encoding *Pseudomonas* plasmids have high similarities to the
213 previously described large plasmids pND6-2 from *Pseudomonas putida* ND6 and pS04-90
214 from *Pseudomonas aeruginosa* S04-90 (16, 17). Both these plasmids lack the putative mobile
215 genetic element that encodes TRIS degradation (**Fig. 3A, Suppl. Fig. S4**). However, pS04-90
216 carries a carbapenem resistance-encoding class 1 integron at almost the same site in the pND6-

217 2 backbone as the TRIS degradation-encoding elements in the *Pseudomonas* plasmids. Both
218 pND6-2 and pS04-90 are conjugative plasmids that can be transferred from their hosts into
219 other *Pseudomonas* strains. Like pND6-2 and pS04-90, p1_Teo1 and its homologs carry genes
220 encoding type IV pili and a type IVB secretion system (**Fig. 3A, Suppl. Fig. S4**), suggesting
221 that these plasmids are also conjugative plasmids. To test this, we set up conjugation
222 experiments with strain Teo1 and strain Teo8 as plasmid donors and *Pseudomonas putida*
223 KT2440 as a non-TRIS-degrading recipient. To be able to differentiate between donor and
224 recipient cells, we labelled strain KT2440 with a chromosomally integrated gentamycin
225 resistance associated with a yellow fluorescent protein (YFP) gene. After the conjugation of
226 Teo1 and Teo8 with strain KT2440::*eyfp-gm* growth of fluorescing colonies was observed on
227 gentamycin-containing minimal medium plates with TRIS as only carbon and nitrogen source
228 (**Fig. 4A**), suggesting that conjugational transfer of the p1_Teo1 and p2_Teo8 plasmids also
229 transferred the ability to use TRIS as growth substrate to KT2440::*eyfp-gm*. The resulting
230 transconjugants were also able to grow with TRIS in liquid culture (**Fig. 4D**), confirming that
231 both gene clusters together encode the complete degradation pathway sufficient to use TRIS as
232 sole carbon and nitrogen source.
233
234

235 ## Discussion

236

237 In this study we identify and characterize a degradation pathway for the synthetic buffer
238 compound TRIS in several *Pseudomonas* strains and a *Shinella* strain, which were all isolated
239 from wastewater purification systems with TRIS as only carbon source. Our results suggest
240 that TRIS degradation proceeds via a pathway that originated recently via a combination of
241 genes from different, formerly independent metabolic pathways and their assembly into two
242 co-regulated gene clusters within a mobile genetic element. Although not all individual
243 functions for the proteins encoded in clusters I and II were biochemically confirmed,
244 conjugational transfer of the plasmid that contains both clusters into *P. putida* KT2440 co-
245 transferred the ability to degrade TRIS, confirming that they together encode the complete
246 degradation pathway sufficient to use TRIS as sole carbon and nitrogen source.

247 TRIS has long been considered biologically inert, because the bonding of its amino
248 group to a tertiary carbon atom prevents its metabolism via transamination or oxidative
249 deamination, which are the most common reactions in the degradation of amines. However,
250 bacterial degradation of α-amino acids with a tertiary α-carbon atom is known for a long time
251 and has been demonstrated for 2-hydroxymethylserine via a tetrahydrofolate-dependent
252 methylserine hydroxymethyltransferase (mSHMT) with D-serine and formaldehyde as
253 products (18). All of our TRIS-degrading isolates encode a protein in cluster II with highest
254 similarities to confirmed D-amino acid-producing mSHMTs (19) as well as a protein for the
255 degradation of D-serine to pyruvate, suggesting that these proteins together can catalyze the
256 degradation of 2-hydroxymethylserine, the product of TRIS oxidation by the TopAB proteins.
257 Thus, we propose a pathway for the catabolism of TRIS, in which TRIS is translocated into the
258 cytoplasm by the TRIS uptake protein TupA and subsequently oxidized to 2-
259 hydroxymethylserine by the TRIS dehydrogenase TopA and the TRIS-aldehyde
260 dehydrogenase TopB via a suspected aldehyde intermediate (**Fig. 5**). 2-Hydroxymethylserine
261 is further transformed into D-serine by the mSHMT protein, which is then transformed into
262 pyruvate by the D-serine dehydratase. The latter can be channelled into the tricarboxylic acid
263 cycle via oxidative decarboxylation to acetyl-CoA. The formaldehyde-accepting
264 tetrahydrofolate (THF) cofactor of the mSHMT protein can then be recycled by the
265 bifunctional methylenetetrahydrofolate dehydrogenase/ methenyltetrahydrofolate
266 cyclohydrolase FolD and the formyltetrahydrofolate deformylase PurU encoded in cluster II
267 (20, 21).

268 The genetic context of the *tupA*, *topA* and *topB* genes is not found outside of cluster I,
269 suggesting that these genes were assembled from multiple origins. The TopA proteins have
270 highest similarities to choline dehydrogenases (CDH), which catalyse the oxidation of choline
271 into betaine aldehyde (22) and belong to the glucose-methanol-choline oxidoreductase family
272 (GMC). Within a phylogenetic GMC protein tree, the TopA proteins form a distinct clade that
273 diverges from the CDH sequences with strong bootstrap support, suggesting that the TRIS
274 dehydrogenase functionality evolved from enzymes with choline dehydrogenase activity.
275 Strikingly, two CDH proteins encoded outside of gene cluster I in *S. zoogloeoides* Teo12
276 cluster basal to the TopA protein clade, suggesting that they could be ancestral to TopA. It is
277 tempting to speculate that the TopA proteins have originated in *Shinella* or a similar organism
278 through the duplication and mutation of CDH-encoding genes. TupA and TopB have highest
279 similarities to proteins involved in the degradation of polyamines like putrescine (23, 24),
280 suggesting that these proteins were recruited from bacterial polyamine degradation pathways
281 (25). The fact that Teo1 was not able to use other α-substituted amino alcohols such as 2-
282 amino-2-methylpropanol and 2-amino-2-methylproandiol as growth substrates suggests that
283 either the substrate uptake by TupA or the oxidation reactions catalysed by TopAB evolved to
284 be highly specific for TRIS.
285 Expression of *tupA* was strictly required for TRIS transformation in *E. coli* cells,
286 suggesting that TRIS translocation is required for TRIS uptake in Gram-negative cells. With a
287 pKa of 8.07 TRIS is mainly positively charged at neutral and acidic pH, preventing its diffusion
288 across the cytoplasmic membrane. The absence of a *tupA* gene homolog in *S. zoogloeoides*
289 Teo12 suggests that this gene was recruited later to the pathway. It remains unknow how TRIS
290 is translocated by Teo12, however, alternative putrescine uptake transporters (23) are also
291 encoded in the genome of Teo12, which might play a role in TRIS uptake in this strain.
292 The genetic context of the genes encoded in cluster II is also present in other
293 *Pseudomonas* strains that do not encode cluster I, suggesting that this gene cluster may have
294 been assembled prior to its recruitment into the TRIS degradation pathway. While SHMT and
295 mSHMT proteins are often accompanied by THF co-factor recycling proteins (19, 26), their
296 genetic association with D-amino acid degradation genes such as the D-serine dehydratase
297 genes in cluster II in a putative operon was not reported so far. In pathogenic bacteria, D-serine
298 dehydratase genes play important roles in the detoxification and catabolism of D-amino acids
299 (27, 28). Thus, we conclude that the second part of the TRIS degradation pathway was
300 assembled by a combination of genes involved in the transformation of α-substituted amino
301 acids and in the degradation of D-amino acids. The presence of mostly incomplete insertion

302 elements up- and downstream of the TRIS degradation gene clusters suggests that the whole
303 DNA segment was originally able to be mobilized as a composite transposon, allowing its
304 transposition between plasmids and the chromosome. The finding of an additional transposase
305 gene between the two gene clusters in *Shinella* and the closely related *Rhizobium* strain
306 corroborates our hypothesis that the pathway was assembled from two independent reactions
307 sequences encoded in clusters I and II.

308 TRIS is used in countless applications in research, industry, medicine, and household
309 settings. Its most prominent applications include its use as a buffer in molecular biology and
310 biochemistry labs, as an excipient in drug formulations, and as an active agent for the treatment
311 of metabolic acidosis and an enhancer for antibiotics and antiseptics for the treatment of Gram-
312 negative infections. Based on its first large scale production in the middle of the twentieth
313 century (29, 30), we hypothesize that the TRIS degradation pathway evolved within the last
314 thirty to fifty years, which is corroborated by the fact that TRIS degradation was not discovered
315 earlier despite its intense use in research laboratories. However, the organization of the TRIS
316 degradation genes in two compact gene clusters and the fact that expression of these
317 presumable operons was regulated in response to TRIS in strain Teo1 are signs for a highly
318 evolved pathway (5), suggesting its turn-around in the environment for a while. The regulator
319 gene between the two clusters is presumably involved in this regulation. Its protein product is
320 similar to the transcription factor GltC that regulates glutamate synthase expression in *Bacillus*
321 *subtilis* (31). The first reports of bacteria being able to utilize TRIS as a growth substrate were
322 published thirty years ago from a group in Spain (32), however, no genetic or biochemical
323 analyses followed this observation.

324 Specific microbial habitats such as sinks and wastewater treatment facilities of large
325 research laboratories, hospitals, or from the TRIS-manufacturing industry could be locations
326 where the TRIS degradation pathway might have originated. First, such habitats encounter
327 significant TRIS concentrations on a regular basis. For example, the antibiotic fosfomycin,
328 which is produced and administered as a TRIS salt, was found at concentrations of 0.13 mM
329 in the influent and 0.015 mM in the effluent of a wastewater treatment plant of a fosfomycin
330 production plant (33), suggesting the presence of similar concentrations of its counterion TRIS.
331 Second, sinks and water purification systems are hotspots for horizontal gene transfer (11, 34,
332 35), which additionally favors the evolution of novel catabolic pathways.

333 The identification of identical TRIS degradation gene clusters in bacteria that have been
334 isolated in Germany, the Republic of Korea, and in China corroborates our findings, that TRIS
335 degradation-encoding plasmids can be readily transferred among bacteria by conjugation-

driven HGT. Our isolation studies suggest that the TRIS degradation pathway is frequently present in the microbiome of municipal wastewater treatment plants but less frequent in freshwater habitats, indicating that environments with high carbon and nitrogen loads better support the maintenance and dissemination of the TRIS degradation pathway than more oligotrophic environments. Although the average TRIS concentration in the sampled wastewater treatment plants is presumably very low, its metabolism as an additional nitrogen and carbon source alongside other recalcitrant molecules might provide sufficient positive selection pressure for bacteria with broad substrate ranges such as *Pseudomonas* and *Shinella* (36–39) to maintain the pathway. Our results corroborate the importance of HGT and mobile genetic elements in the evolution of novel catabolic pathways. With this, they provide additional knowledge about the basic structure of such elements, which can be used for future use in engineering bacteria for bioaugmentation (11).

350 # Experimental procedures

351 ## Targeted enrichment and growth cultures

352 TRIS-degrading strains were isolated and grown in a phosphate-buffered minimal medium (pH
353 7.0) containing 0.01 mM $CaCl_2$ x 2 H_2O, 1.5 mM $MgSO_4$ x 7 H_2O, 35 mM K_2HPO_4 x 3 H_2O,
354 15 mM NaH_2PO_4 x H_2O, trace elements and 10 mM TRIS. For solid media plates, 1.5 % agar
355 was added prior to autoclaving. Enrichment cultures (5 ml) were inoculated with fresh samples
356 (1 ml) from local wastewater treatment plants (activated sludge or activated carbon), a water
357 purification plant (activated carbon), or different freshwater habitats (**Supp. Tab. ST1**). When
358 enrichment cultures showed growth, 100 µl of the culture supernatant were transferred to 5 ml
359 fresh minimal medium with TRIS, and this was repeated two to three times before cultures
360 were spread onto solid minimal medium plates containing to isolate individual TRIS-degrading
361 colonies. Growth experiments in liquid cultures were carried out at 30°C and 200 rpm in 1 ml
362 or 5 ml medium in 24-well plates or in reaction tubes, respectively. Experimental cultures were
363 inoculated from washed, over-night starter cultures grown with TRIS. Growth was followed
364 by measuring the optical density at 600 nm (OD_{600}). For transcriptome experiments, TRIS was
365 replaced with 20 mM pyruvate and 20 mM NH_4Cl were added as nitrogen source. For substrate
366 tests, TRIS was replaced with 10 mM D- or L-serine, 10 mM choline, 10 mM betaine, 10 mM
367 2-amino-2-methylpropanol, 10 mM 2-amino-2-methylproandiol, 10 mM sarcosine, or 10 mM
368 serinol, and 20 mM NH_4Cl were added as nitrogen source. *Pseudomonas putida* KT2440 and
369 its derivatives were grown in the same minimal medium with succinate as carbon source at
370 30°C. *E. coli* strains were grown in half-concentrated lysogeny broth (LB) at 37°C. LB grown
371 overnight E. *coli* cultures carrying predicted TRIS degradation genes on the expression vector
372 pUCp18 were inoculated into fresh LB medium and 0.2 mM (isopropyl β-D-1-
373 thiogalactopyranoside) IPTG were added at an OD_{600} of around 0.4. Cultures were grown to a
374 final OD_{600} of 0.8 – 1.0 before cells were harvested, washed with sterile minimal medium
375 without carbon source, and were resuspended in minimal medium with TRIS to an OD_{600} of
376 1.5. If required, kanamycin (20-50 µg/ml), tetracycline (10 µg/ml), or gentamycin (20-40
377 µg/ml) antibiotics were added to the medium after autoclaving. To test whether 2-
378 hydroxymethylserine can be used as a growth for Teo1, cell suspensions of *tupA*, *topB* and
379 *topA* expressing *E. coli* cells that had produced 2-hydroxymethylserine from TRIS were
380 centrifuged and sterile filtered (0.2 µm) and the culture supernatant was inoculated with strain
381 Teo1 cells.

382 TRIS quantification

383 TRIS, its degradation intermediates, and ammonium were identified and quantified by high
384 performance liquid chromatography (HPLC) coupled to a mass spectrometer and a UV/Vis
385 detector (40) after derivatization of their amino group with diethyl ethoxymethylenemalonate
386 (DEEMM, (41)). For this, 100 µl culture supernatants were mixed with 130 µl borate buffer (1
387 M, pH 9.0), 75 µl methanol, and 3 µl DEEM reagent, followed by 30 min sonication and 60
388 min incubation at 70°C before injection into the HPLC. A gradient (flow rate 0.3 ml/min) of
389 ammonium-acetate buffer (10 mM, pH 3.0, with 0.1 % (v/v) formic acid, eluent A) and
390 acetonitrile (eluent B) were used for product elution starting with 10 % eluent B for 2 min,
391 increasing to 90 % eluent B within 22 min, remaining at 90 % eluent B for 2 min, and returning
392 to 10 % eluent B within 1 min, followed by an equilibration of 5 min. Products were identified
393 based on their mass spectra after electrospray ionization in positive ion mode. The capillary
394 voltage was 2500 V, the end plate offset 500 V and the capillary temperature 300°C. Nebulizer
395 pressure was 22.5 psi, dry gas flow 12 l/min and dry temperature 200°C. Quantification was
396 performed based on the product peak areas at 280 nm UV absorbance, and concentrations were
397 calculated based on concentration curves of authentic standards treated in the same way. The
398 concentration of 2-hydroxymethylserine was calculated using the same standard curve as for
399 TRIS.

400 DNA manipulation

401 DNA amplification and purification was carried out using standard techniques. DNA for
402 cloning purposes was amplified by PCR using a high-fidelity polymerase (Q5, New England
403 Biolabs). Predicted TRIS degradation genes were cloned into the expression plasmid pUCp18
404 (42) by isothermal assembly (43). For this, DNA fragments were PCR-amplified from *P.*
405 *hunanensis* Teo1 DNA and pUCp18 was linearized using primers with overlapping homologies
406 designed with the NEBuilder online tool (New England Biolabs, **Supp. Tab. ST2**). Purified
407 fragments and plasmid were combined in equimolar concentrations in isothermal assembly
408 reaction buffer and assembled at 50°C for 60 min. Assembled DNA was transformed into
409 competent *E. coli* DH5α cells by chemical transformation and positive clones were selected on
410 LB agar plates containing an appropriate antibiotic. Correct insertion of the fragments into the
411 vector was confirmed by PCR using standard M13 primers and sequencing (Microsynth AG,
412 Switzerland). A YFP-tagged *Pseudomonas putida* KT2440 strain was constructed following
413 the protocol from (44) using the plasmid pBK-miniTn7(Gm)PA1/04/03-*eyfp*-a. In short, cells

414 from an overnight culture of *P. putida* KT2440 were mixed with cells of *E. coli* SM10(*λpir*)
415 pUX-BF13, *E. coli* JM105 pBK-miniTn7(Gm)PA1/04/03-*eyfp*-a and *E. coli* RK600 and
416 conjugation was carried out at 30°C over night on non-selective LB plates. Cells were washed
417 of the plates with minimal medium without carbon source and were plated onto minimal
418 medium with 10 mM benzoate and gentamycin to select for positive transconjugants. Single
419 colonies showing YFP fluorescence (Chemidoc MP Imaging System, Bio-Rad Laboratories
420 GmbH) were selected and correct insertion of the *yfp*-containing Tn7 element gene into the
421 chromosome was confirmed by PCR.

422 Transcriptome analysis

423 *P. hunanensis* Teo1 was grown in minimal medium with TRIS as only carbon and nitrogen
424 source or with pyruvate and ammonium and cultures were harvested during mid-log phase.
425 Harvested cells were re-suspended in 800 µl RLT buffer (RNeasy Mini Kit, Qiagen) with β-
426 mercaptoethanol (10 µl ml^{-1}) and cell lysis was performed using a laboratory ball mill.
427 Subsequently, 400 µl RLT buffer (RNeasy Mini Kit Qiagen) with β-mercaptoethanol (10 µl
428 ml^{-1}) and 1200 µl 96% (vol./vol.) ethanol were added. For RNA isolation, the RNeasy Mini Kit
429 (Qiagen) was used as recommended by the manufacturer, but instead of RW1 buffer RWT
430 buffer (Qiagen) was used in order to isolate RNAs smaller than 200 nucleotides also. To
431 determine the RNA integrity number the isolated RNA was run on an Agilent Bioanalyzer
432 2100 using an Agilent RNA 6000 Nano Kit as recommended by the manufacturer (Agilent
433 Technologies, Waldbronn, Germany). Remaining genomic DNA was removed by digesting
434 with TURBO DNase (Invitrogen, Thermo Fischer Scientific, Paisley, UK). The Pan-
435 Prokaryozes riboPOOL kit v4 (siTOOLS BIOTECH, Planegg/Martinsried, Germany) was used
436 to reduce the amount of rRNA-derived sequences. For sequencing, the strand-specific cDNA
437 libraries were constructed with a NEB Next Ultra II Directional RNA library preparation kit
438 for Illumina and the NEB Next Multiplex Oligos for Illumina (New England BioLabs,
439 Frankfurt am Main, Germany). To assess quality and size of the libraries samples were run on
440 an Agilent Bioanalyzer 2100 using an Agilent High Sensitivity DNA Kit as recommended by
441 the manufacturer (Agilent Technologies). Concentration of the libraries was determined using
442 the Qubit dsDNA HS Assay Kit as recommended by the manufacturer (Life Technologies
443 GmbH, Darmstadt, Germany). Sequencing was performed by using the HiSeq2500 instrument
444 (Illumina Inc., San Diego, CA, USA) using the HiSeq Rapid SR Cluster Kit v2 for cluster
445 generation and the HiSeq Raid SBS Kit (50 cycles) for sequencing in the single-end mode and
446 running 1x50 cycles. For quality filtering and removing of remaining adaptor sequences,

447 Trimmomatic-0.39 (Bolger et al., 2014) and a cutoff phred-33 score of 15 were used. The
448 mapping against the reference genomes of *Pseudomonas hunanensis Teo1* (BioProject
449 PRJNA999090, Accessions CP131127- CP131129) was performed with Salmon (v 1.9.0) (45).
450 As mapping back-bone a file that contains all annotated transcripts excluding rRNA genes and
451 the whole genome of the references as decoy was prepared with a k-mer size of 11. Decoy-
452 aware mapping was done in selective-alignment mode with '–mimicBT2', '–
453 disableChainingHeuristic' and '–recoverOrphans' flags as well as sequence and position bias
454 correction and 10,000 bootstraps. For –fldMean and –fldSD, values of 325 and 25 were used,
455 respectively. The quant.sf files produced by Salmon were subsequently loaded into R (v 4.2.0)
456 using the tximport package (v 1.24.0). DeSeq2 (v 1.36.0) (46) was used for normalization of
457 the reads and fold change shrinkages were also calculated with DeSeq2 and the apeglm package
458 (v 1.18.0) (47). Genes with a $\log_2$-foldchange of +2/-2 and a p-adjust value <0.05 were
459 considered differentially expressed. Raw reads have been deposited in the Sequence Read
460 Archive under study SRP451968 (SRR25447477-SRR25447482).

461 Conjugation experiments

462 Conjugation experiments were carried out using strains Teo1 and Teo8 as donors and
463 gentamicin-resistant *P. putida* KT2440::*eyfp-gm* as recipients. Approximately 1 x 10^9 donor
464 cells and 3 x 10^9 recipient cells were mixed and spotted onto sterile cellulose acetate filter disks
465 (ca. 3 cm^2, 0.45 µm pores) on LB agar plates. Conjugation plates were incubated at 30°C for
466 24 h before cells were washed off the filter disks with 50 mM phosphate buffer (pH 7.2).
467 Decimal dilutions were plated onto minimal medium agar plates with TRIS as only carbon and
468 nitrogen source containing 40 µg/ml gentamicin. Transconjugants were screen using a
469 ChemiDocTM Imaging System (Bio-Rad) using blue epi illumination and an emission filter at
470 530 nm. The conjugation rate was calculated by dividing the number of positive
471 transconjugants by the number of recipient cells in each assay. The successful transfer of the
472 p1_Teo1 and p2_Teo8 plasmids was confirmed by colony PCR amplifying the *tupA*, *topA*,
473 *topB*, *glyA*, and *dsdA* genes (**Suppl. Tab. ST2**).
474

Acknowledgment

The authors like to thank the operators and the employs of the water treatment facilities in the cities of Münster, Hamm, Dülmen, and Güthersloh-Putzhagen for their help with sampling. We like to especially thank Rudolf Cigelski (Hamm) for his continued support and his great efforts to provide us with samples. We further thank Malte Jochimsen and Anna Hannes for experimental support.

Data availability

The whole-genome shotgun projects have been deposited at DDBJ/ENA/GenBank under the BioProject accession numbers PRJNA999090, PRJNA999091, PRJNA999092, PRJNA999094, PRJNA999097, PRJNA999137, PRJNA999141 and the transcriptome data under the BioProject accession number PRJNA999090 with the SRA accession numbers SRR25447477 - SRR25447482.

References

1. B. A. Kolvenbach, D. E. Helbling, H.-P. E. Kohler, P. F.-X. Corvini, Emerging chemicals and the evolution of biodegradation capacities and pathways in bacteria. *Curr. Opin. Biotechnol.* **27**, 8–14 (2014).

2. S. D. Copley, Evolution of efficient pathways for degradation of anthropogenic chemicals. *Nat. Chem. Biol.* **5**, 559–566 (2009).

3. N. Udiković-Kolić, C. Scott, F. Martin-Laurent, Evolution of atrazine-degrading capabilities in the environment. *Appl. Microbiol. Biotechnol.* **96**, 1175–1189 (2012).

4. E. M. Top, D. Springael, N. Boon, Catabolic mobile genetic elements and their potential use in bioaugmentation of polluted soils and waters. *FEMS Microbiol. Ecol.* **42**, 199–208 (2002).

5. G. R. Johnson, J. C. Spain, Evolution of catabolic pathways for synthetic compounds: bacterial pathways for degradation of 2,4-dinitrotoluene and nitrobenzene. *Appl. Microbiol. Biotechnol.* **62**, 110–123 (2003).

6. M. Aulestia, A. Flores, S. Acosta-Jurado, E. Santero, E. M. Camacho, Genetic Characterization of the Ibuprofen-Degradative Pathway of *Rhizorhabdus wittichii* MPO218. *Appl. Environ. Microbiol.* **88**, e00388-22 (2022).

7. M. L. Bonatelli, *et al.*, Recently evolved combination of unique sulfatase and amidase genes enables bacterial degradation of the wastewater micropollutant acesulfame worldwide. *Front. Microbiol.* **14**, 14:1223838 (2023).

8. A. B. Rios-Miguel, *et al.*, Microbial paracetamol degradation involves a high diversity of novel amidase enzyme candidates. *Water Res. X* **16**, 100152 (2022).

9. S. D. Copley, Evolution of a metabolic pathway for degradation of a toxic xenobiotic: the patchwork approach. *Trends Biochem. Sci.* **25**, 261–265 (2000).

10. D. Springael, E. M. Top, Horizontal gene transfer and microbial adaptation to xenobiotics: new types of mobile genetic elements and lessons from ecological studies. *Trends Microbiol.* **12**, 53–58 (2004).

11. A. B. Rios Miguel, M. S. M. Jetten, C. U. Welte, The role of mobile genetic elements in organic micropollutant degradation during biological wastewater treatment. *Water Res. X* **9**, 100065 (2020).

12. R. P. Schwarzenbach, *et al.*, The challenge of micropollutants in aquatic systems. *Science* **313**, 1072–1077 (2006).

13. B. Petrie, R. Barden, B. Kasprzyk-Hordern, A review on emerging contaminants in wastewaters and the environment: Current knowledge, understudied areas and recommendations for future monitoring. *Water Res.* **72**, 3–27 (2015).

14. J. Benner, *et al.*, Is biological treatment a viable alternative for micropollutant removal in drinking water treatment processes? *Water Res.* **47**, 5955–5976 (2013).

525 15. M. Herrero, D. C. Stuckey, Bioaugmentation and its application in wastewater treatment:
526 A review. *Chemosphere* **140**, 119–128 (2015).

527 16. A. van der Zee, *et al.*, Spread of carbapenem resistance by transposition and conjugation
528 among *Pseudomonas aeruginosa*. *Front. Microbiol.* **9**, 2057 (2018).

529 17. S. Wang, S. Li, D. Du, D. Wang, W. Yan, Conjugative transfer of megaplasmids pND6–1
530 and pND6–2 enhancing naphthalene degradation in aqueous environment:
531 characterization and bioaugmentation prospects. *Appl. Microbiol. Biotechnol.* **104**, 861–
532 871 (2020).

533 18. E. M. Wilson, E. E. Snell, Metabolism of α-methylserine. *J. Biol. Chem.* **237**, 3171–3179
534 (1962).

535 19. H. Nozaki, S. Kuroda, K. Watanabe, K. Yokozeki, Cloning of the gene encoding α-
536 methylserine hydroxymethyltransferase from *Aminobacter* sp. AJ110403 and *Ensifer* sp.
537 AJ110404 and characterization of the recombinant enzyme. *Biosci. Biotechnol. Biochem.*
538 **72**, 3002–3005 (2008).

539 20. L. D'Ari, J. C. Rabinowitz, Purification, characterization, cloning, and amino acid
540 sequence of the bifunctional enzyme 5,10-methylenetetrahydrofolate
541 dehydrogenase/5,10-methenyltetrahydrofolate cyclohydrolase from *Escherichia coli*. *J.*
542 *Biol. Chem.* **266**, 23953–23958 (1991).

543 21. P. L. Nagy, A. Marolewski, S. J. Benkovic, H. Zalkin, Formyltetrahydrofolate hydrolase,
544 a regulatory enzyme that functions to balance pools of tetrahydrofolate and one-carbon
545 tetrahydrofolate adducts in *Escherichia coli*. *J. Bacteriol.* **177**, 1292–1298 (1995).

546 22. M. J. Wargo, Homeostasis and catabolism of choline and glycine betaine: Lessons from
547 *Pseudomonas aeruginosa*. *Appl. Environ. Microbiol.* **79**, 2112–2120 (2013).

548 23. S. Krysenko, W. Wohlleben, Polyamine and ethanolamine metabolism in bacteria as an
549 important component of nitrogen assimilation for survival and pathogenicity. *Med. Sci.*
550 **10**, 40 (2022).

551 24. J. M. Luengo, E. R. Olivera, Catabolism of biogenic amines in *Pseudomonas* species.
552 *Environ. Microbiol.* **22**, 1174–1192 (2020).

553 25. N. Nemoto, *et al.*, Mechanism for regulation of the putrescine utilization pathway by the
554 transcription factor PuuR in *Escherichia coli* K-12. *J. Bacteriol.* **194**, 3437–3447 (2012).

555 26. S. Shetty, U. Varshney, Regulation of translation by one-carbon metabolism in bacteria
556 and eukaryotic organelles. *J. Biol. Chem.* **296**, 100088 (2021).

557 27. J. P. R. Connolly, A. J. Roe, When and where? Pathogenic *Escherichia coli* differentially
558 sense host D-serine using a universal transporter system to monitor their environment.
559 *Microb. Cell* **3**, 181–184 (2016).

560 28. G. Li, C.-D. Lu, The cryptic *dsdA* gene encodes a functional d-serine dehydratase in
561 *Pseudomonas aeruginosa* PAO1. *Curr. Microbiol.* **72**, 788–794 (2016).

562 29. J. Bourguignon, M.-X. Sion, M. Moreau, Preparation of
563 Tris(hydroxymethyl)aminomethane. US Patent No. US4233245A, U.S. Patent and
564 Trademark Office (1980).

565 30. G. W. McMillan, Electrolytic production of aminoalcohols. US Patent No. US2485982A,
566 U.S. Patent and Trademark Office (1949).

567 31. D. E. Bohannon, A. L. Sonenshein, Positive regulation of glutamate biosynthesis in
568 *Bacillus subtilis*. *J. Bacteriol.* **171**, 4718–4727 (1989).

569 32. J. Fábregas, V. Vázquez, B. Cabezas, A. Otero, Tris not only controls the pH in microalgal
570 cultures, but also feeds bacteria. *J. Appl. Phycol.* **5**, 543–545 (1993).

571 33. P. Zeng, *et al.*, Ion chromatography as highly suitable method for rapid and accurate
572 determination of antibiotic fosfomycin in pharmaceutical wastewater. *Water Sci. Technol.*
573 **69**, 2014–2022 (2014).

574 34. K. Abe, N. Nomura, S. Suzuki, Biofilms: hot spots of horizontal gene transfer (HGT) in
575 aquatic environments, with a focus on a new HGT mechanism. *FEMS Microbiol. Ecol.*
576 **96**, fiaa031 (2020).

577 35. L. Diorio-Toth, *et al.*, Intensive care unit sinks are persistently colonized with multidrug
578 resistant bacteria and mobilizable, resistance-conferring plasmids. *mSystems*, e00206-23
579 (2023).

580 36. E. R. B. Moore, *et al.*, "Nonmedical: *Pseudomonas*" in *The Prokaryotes*, M. Dworkin, S.
581 Falkow, E. Rosenberg, K.-H. Schleifer, E. Stackebrandt, Eds. (Springer New York, 2006),
582 pp. 646–703.

583 37. H. J. Jiang, Y. Ma, G. J. Qiu, F. L. Wu, S. L. Chen, Biodegradation of nicotine by a novel
584 Strain *Shinella* sp. HZN1 isolated from activated sludge. *J. Environ. Sci. Health Part B*
585 **46**, 703–708 (2011).

586 38. C. Hesse, *et al.*, Genome-based evolutionary history of *Pseudomonas* spp. *Environ.*
587 *Microbiol.* **20**, 2142–2159 (2018).

588 39. Y. Huang, Z. Yu, L. Liu, Y. Che, T. Zhang, Acesulfame anoxic biodegradation coupled to
589 nitrate reduction by enriched consortia and isolated *Shinella* spp. *Environ. Sci. Technol.*
590 (2022) https:/doi.org/10.1021/acs.est.2c03656 (July 21, 2023).

591 40. J. Holert, *et al.*, Identification of bypass reactions leading to the formation of one central
592 steroid degradation intermediate in metabolism of different bile salts in *Pseudomonas* sp.
593 strain Chol1. *Environ. Microbiol.* **8**, 3373–3389 (2016).

594 41. M. Alaiz, J. L. Navarro, J. Girón, E. Vioque, Amino acid analysis by high-performance
595 liquid chromatography after derivatization with diethyl ethoxymethylenemalonate. *J.*
596 *Chromatogr. A* **591**, 181–186 (1992).

597 42. H. P. Schweizer, *Escherichia-Pseudomonas* shuttle vectors derived from pUC18/19. *Gene*
598 **97**, 109–121 (1991).

599 43. D. G. Gibson, *et al.*, Enzymatic assembly of DNA molecules up to several hundred
600 kilobases. *Nat. Methods* **6**, 343–345 (2009).

601 44. M. Klausen, *et al.*, Biofilm formation by *Pseudomonas aeruginosa* wild type, flagella and
602 type IV pili mutants: Roles of bacterial motility in the formation of the flat *P. aeruginosa*
603 biofilm. *Mol. Microbiol.* **48**, 1511–1524 (2003).

604 45. R. Patro, G. Duggal, M. I. Love, R. A. Irizarry, C. Kingsford, Salmon provides fast and
605 bias-aware quantification of transcript expression. *Nat. Methods* **14**, 417–419 (2017).

606 46. M. I. Love, W. Huber, S. Anders, Moderated estimation of fold change and dispersion for
607 RNA-seq data with DESeq2. *Genome Biol.* **15**, 550 (2014).

608 47. A. Zhu, J. G. Ibrahim, M. I. Love, Heavy-tailed prior distributions for sequence count data:
609 removing the noise and preserving large differences. *Bioinformatics* **35**, 2084–2092
610 (2019).

611

612

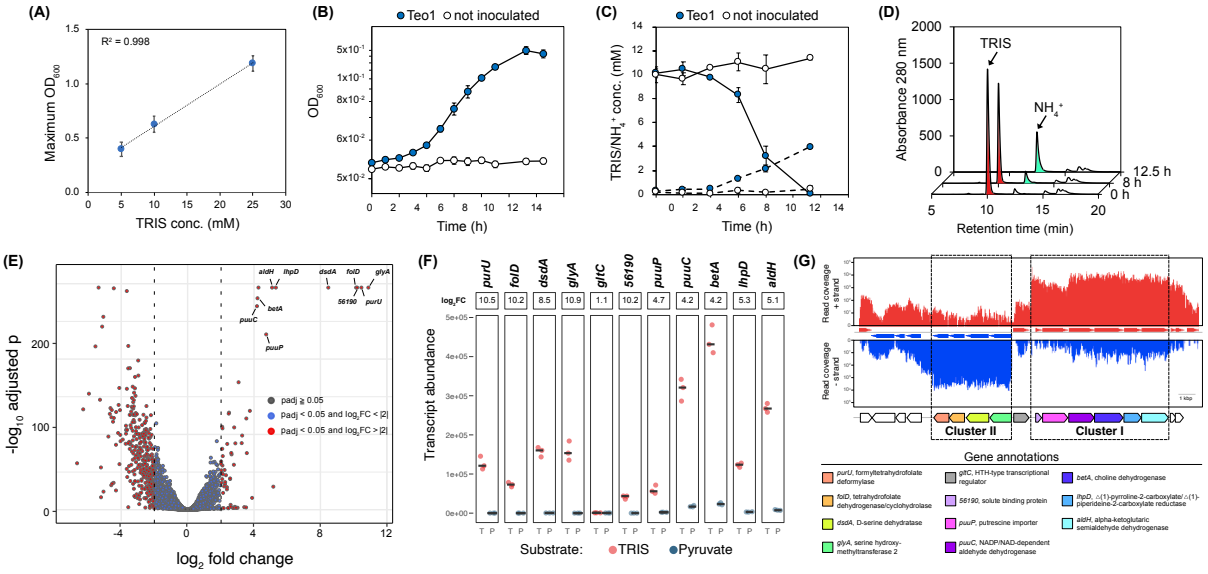

Fig. 1: Characteristics of TRIS metabolism in *Pseudomonas hunanensis* Teo1 and identification of potential TRIS degradation genes. (**A**) Maximal biomass production of strain Teo1 in relation to TRIS concentration. Error bars indicate standard deviation (n = 3). (**B**) Growth of strain Teo1 with 10 mM TRIS as only carbon and nitrogen source. (**C**) Removal of TRIS (straight lines) and formation of ammonium (dashed lines) in Teo1 growth cultures. (**D**) Representative HPLC chromatograms of a strain Teo1 culture growing with 10 mM TRIS. TRIS is depleted from the culture while ammonium is released. (**E**) Volcano plot of transcriptome data showing significantly up-regulated genes (red) under TRIS-grown (positive fold changes) and pyruvate-grown conditions (negative fold changes) in Teo1. Genes predicted to be involved in TRIS degradation are labelled. (**F**) Transcript abundances and $\log_2$(fold changes) of the predicted TRIS degradation genes in Teo1 in TRIS- and pyruvate-grown cells (three biological replicates of each growth substrate, horizontal bar indicates median, corrected p values of all selected genes were < 0.05). (**G**) mRNA reads (red: positive strand, blue: negative strand) of a representative TRIS-grown culture mapped onto the DNA section containing the predicted TRIS degradation gene clusters in strain Teo1.

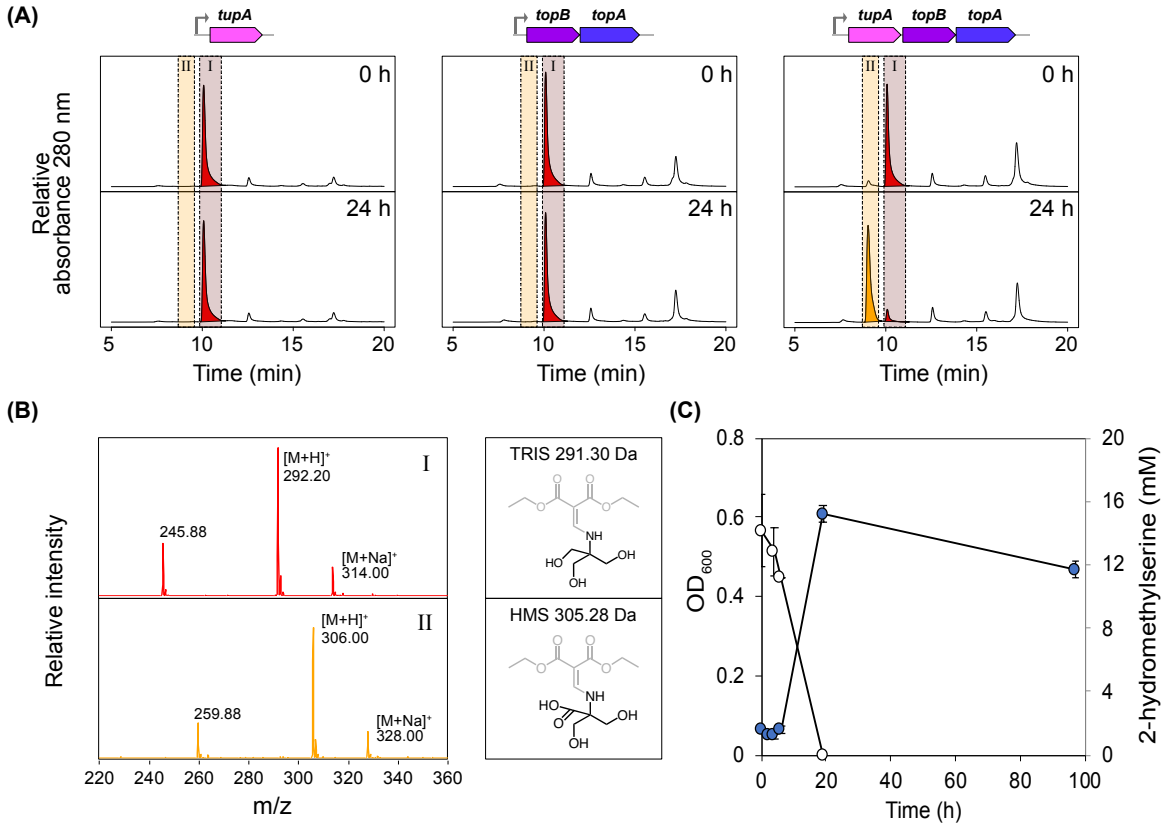

Fig. 2: TRIS transformation activity of *E. coli* strains carrying different combinations of the putrescine importer-like protein-encoding gene (*puuP,* now *tupA*), the aldehyde dehydrogenase-encoding gene (*puuC,* now *topB*), and the choline dehydrogenase-like protein-encoding gene (*betA,* now *topA*) on the expression plasmid pUCp18. (**A**) Representative HPLC-UV/Vis chromatograms of TRIS-containing cell suspension supernatants of *E. coli* strains that carried either the *tupA* gene, the *topB* and *topA* genes, or all three genes. TRIS (peak I, red) was transformed into a new compound (peak II, orange) in the *E. coli* strain that carries all three genes only. The cloned genes were under the activity of the *lac* promotor (grey arrow). (**B**) Mass spectra of TRIS (peak I) and the new product (peak II). The new product was identified as 2-hydroxymethylserine based on the molecular mass of its diethyl ethoxymethylenemalonate (DEEMM, grey molecule moiety) derivative of 305 Da, which is 14 Da heavier than the molecular mass of 291 Da of the DEEMM derivative of TRIS. (**C**) Growth of strain Teo1 (blue circles) in sterilized culture supernatants containing 2-hydroxymethylserine produced from TRIS and removal of 2-hydroxymethylserine (white circles). Average and standard deviation of three independent biological replicates are shown.

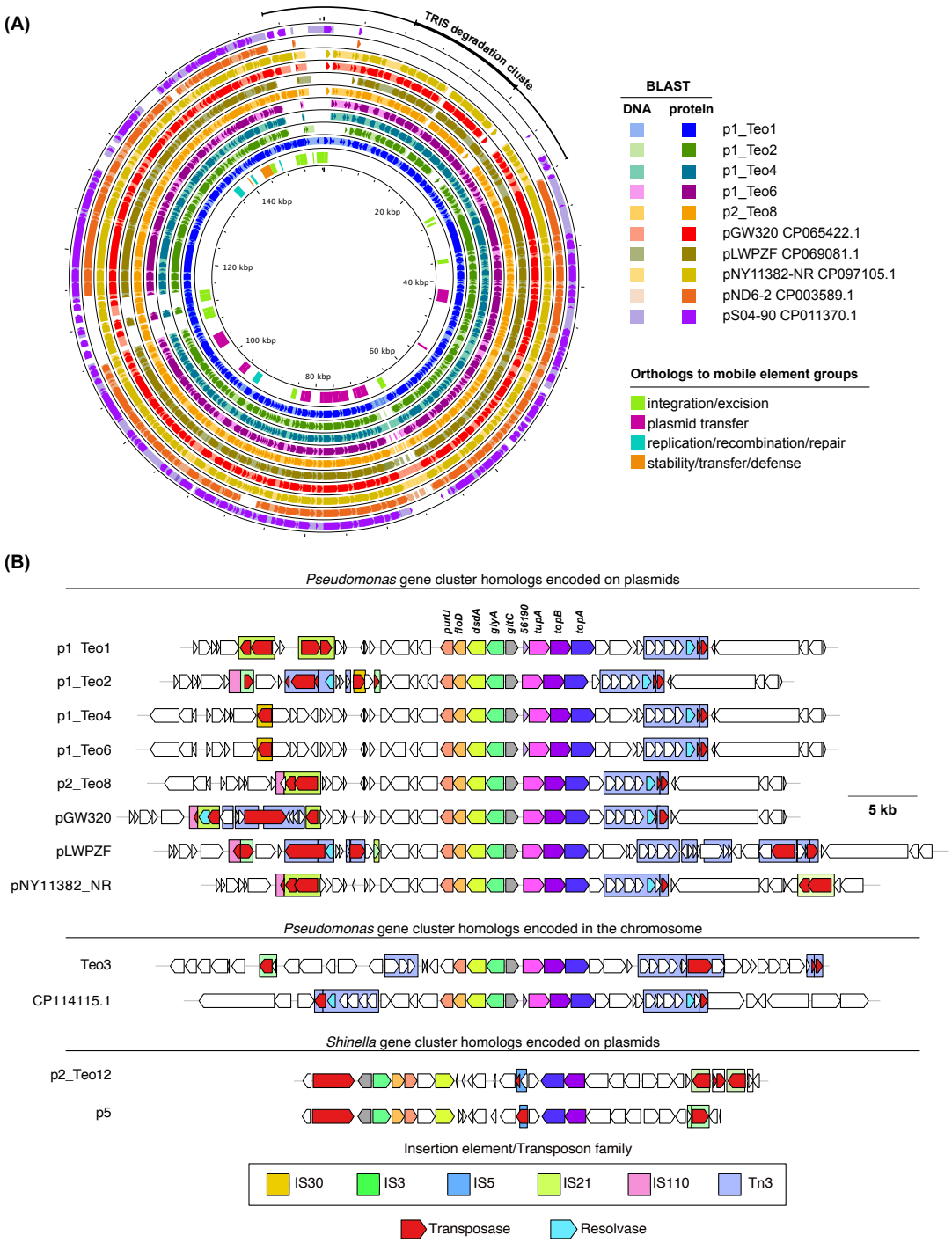

Fig: 3: TRIS degradation gene clusters in the genomes of the sequenced TRIS-degrading isolates from this study and of homologous gene clusters found in the NCBI nr nucleotide database. (**A**) Most TRIS degradation gene clusters are located on large circular plasmids with high sequence similarities to the *Pseudomonas* plasmids pND6-2 and pS04-90, which lack the TRIS degradation clusters. The outer black line indicates the location of the putative mobile genetic element including the TRIS degradation genes. Like pND6-2 and pS04-90, the TRIS degradation-encoding plasmids encode orthologs to mobile elements groups (inner circle) including a type IVB secretion system and a type IV pilus for plasmid transfer as well as a type II toxin-antitoxin system. (**B**) All TRIS degradation gene clusters, including plasmid- and chromosome-encoded clusters, are flanked upstream and downstream by transposon- or insertion element-like structures. The plasmid p2_Teo12 from *Shinella* sp. strain Teo12 and the homologous plasmid p5 in a *Rhizobium* strain have no similarity to the other TRIS degradation-encoding plasmids, but also carry two gene clusters which encode homologs to the other TRIS degradation proteins.

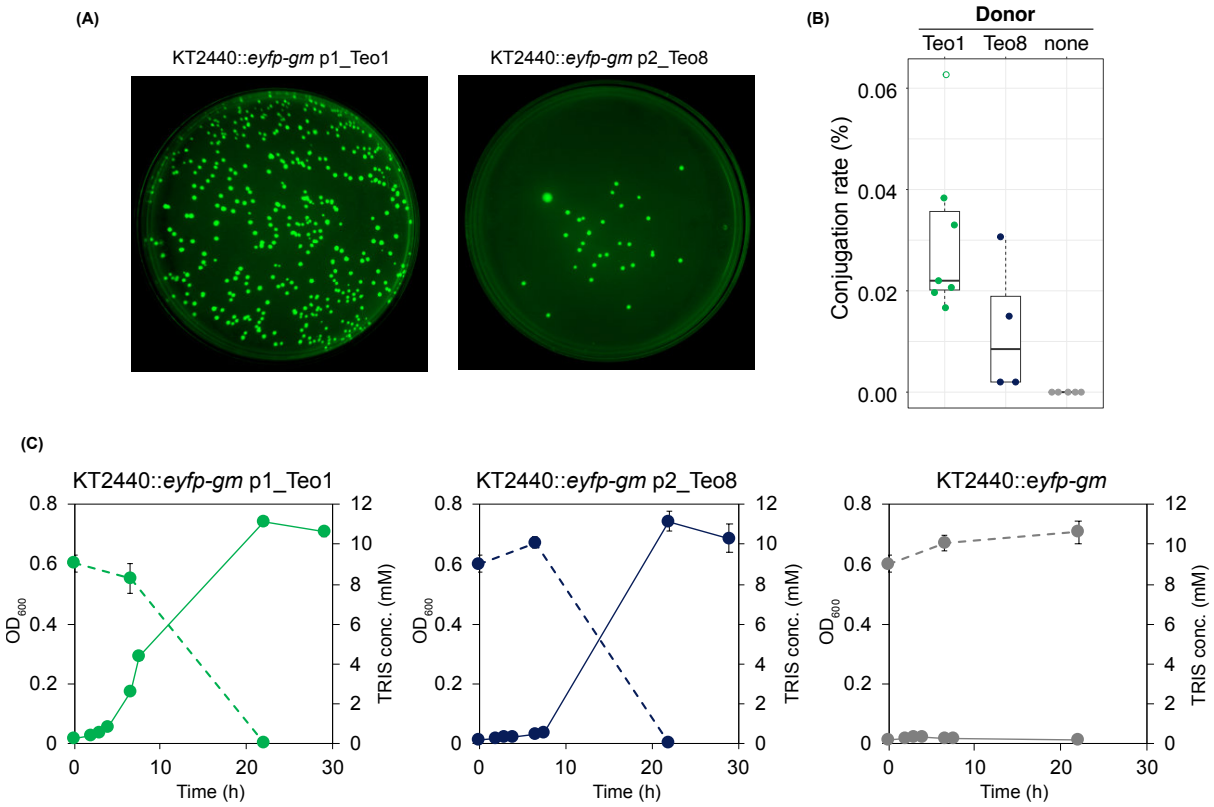

Fig. 4: Conjugative transfer of the TRIS degradation pathway-encoding plasmids p1_Teo1 and p2_Teo8. (**A**) Growth of YFP-fluorescing colonies on TRIS-containing agar plates after conjugation of *P. putida* KT2440::*eyfp-gm* with Teo1 (left panel) and Teo8 (right panel) as donor strains. (**B**) Conjugation rate of KT2440::*eyfp-gm* with p1_Teo1, p2_Teo8, and of a control without donor cells. Black lines indicate median rates of three independent conjugation experiments, boxes indicate the interquartile range, and dashed lines the maximum and minimum range. Transconjugants of up to seven replicates from three independent experiments were counted. Datapoints are coloured based on the donor strain. Outliers are not filled. (**C**) Degradation of TRIS (dashed lines) and growth (solid lines) of *P. putida* KT2440::*eyfp-gm* p1_Teo1 and p2_Teo8 transconjugants in liquid medium. The recipient strain *P. putida* KT2440::*eyfp-gm* without the conjugated plasmids was neither able to grow with, nor to degrade TRIS.

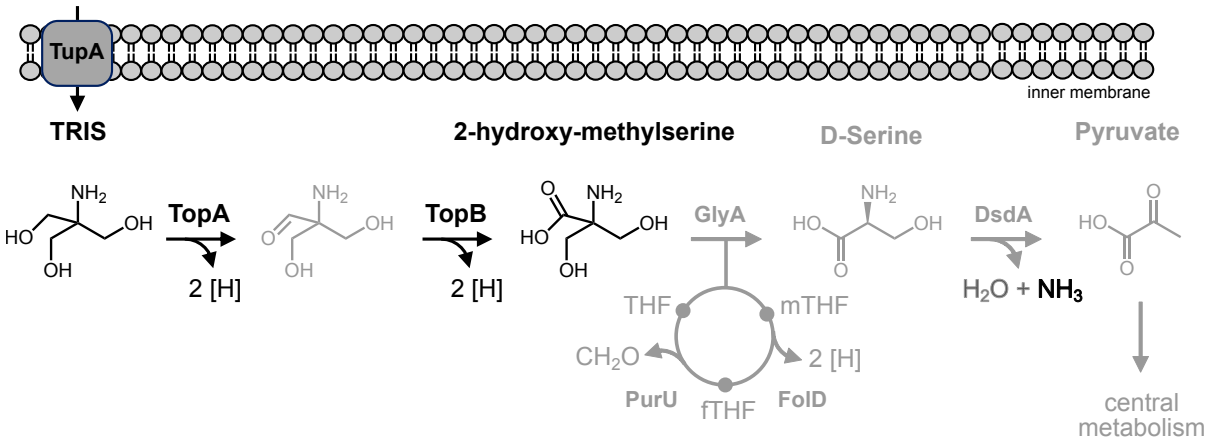

Fig. 5: Proposed TRIS degradation pathway. Confirmed reactions and intermediates are in black, proposed reactions and intermediates are in grey, THF = tetrahydrofolate, mTHF = methenyltetrahydrofolate, fTHF = formyltetrahydrofolate.

670 **Tab. 1**: Genes potentially involved in TRIS degradation in *Pseudomonas hunanensis* Teo1.

Gene	Locus tag	Annotated function	Confirmed function and new gene ID	Protein family (InterProScan)	Best hit (Swiss-Prot)	% identity	
purU	PshuTeo1_ 56140	Formyltetrahydrofolate deformylase		Formyltetrahydrofolate deformylase (IPR004810)	Q46339, Formyltetrahydrofolate deformylase, *Corynebacterium* sp.	46.8	Cluster II
folD	PshuTeo1_ 56150	Bifunctional protein FolD		Tetrahydrofolate dehydrogenase/ cyclohydrolase (IPR000672)	A6UB98, Bifunctional protein FolD 2, *Sinorhizobium medicae*	73.0	
dsdA	PshuTeo1_ 56160	D-serine dehydratase		D-serine ammonia-lyase (IPR011780)	B3PYT5, Probable D-serine dehydratase, *Rhizobium etli*	66.1	
glyA	PshuTeo1_ 56170	Serine hydroxy-methyltransferase 2		Serine hydroxymethyltransferase (IPR001085)	B2DEU8, 2-methylserine hydroxymethyltransferase, *Aminobacter* sp.	66.6	
gltC	PshuTeo1_ 56180	HTH-type transcriptional regulator		non predicted	P71318, Hydrogen peroxide-inducible genes activator, *Pectobacterium carotovorum*	26.9	
56190	PshuTeo1_ 56190	hypothetical protein		none predicted	P45766, Putative amino-acid ABC transporter-binding protein YhdW, *Escherichia coli*	68.9	Cluster I
puuP	PshuTeo1_ 56200	Putrescine importer	TRIS uptake protein, *tupA*	Amino acid/polyamine transporter I (IPR002293)	P76037, Putrescine importer PuuP, *Escherichia coli*	41.8	
puuC	PshuTeo1_ 56210	NADP/NAD-dependent aldehyde dehydrogenase	TRIS aldehyde dehydrogenase, *topB*	none predicted	P23883, NADP/NAD-dependent aldehyde dehydrogenase PuuC, *Escherichia coli*	46.0	
betA	PshuTeo1_ 56220	Oxygen-dependent choline dehydrogenase	TRIS dehydrogenase, *topA*	Glucose-methanol-choline oxidoreductase (IPR012132)	Q9L4K0, Oxygen-dependent choline dehydrogenase, *Chromohalobacter salexigens*	48.3	
lhpD	PshuTeo1_ 56230	Δ(1)-Pyrroline-2-carboxylate/Δ(1)-piperideine-2-carboxylate reductase		Malate/L-lactate dehydrogenase-like (IPR003767)	Q9I492, Δ(1)-pyrroline-2-carboxylate/Δ(1)-piperideine-2-carboxylate reductase, *Pseudomonas aeruginosa*	67.0	
aldH	PshuTeo1_ 56240	Alpha-ketoglutaric semialdehyde dehydrogenase		Alpha-ketoglutaric semialdehyde dehydrogenase (IPR044151)	Q6FFQ0, Alpha-ketoglutaric semialdehyde dehydrogenase, *Acinetobacter baylyi*	58.5	

671